Available online at www.sciencedirect.com
SCIENCE DIRECT®
International Journal of Heat and Mass Transfer 48 (2005) 2493–2502
International Journal of HEAT and MASS TRANSFER
www.elsevier.com/locate/ijhmt

A simple design of fins for boiling heat transfer

Shih-Pin Liaw [a], Rong-Hua Yeh [b,*], Wen-Tong Yeh [c]

[a] Department of Mechanical and Mechatronic Engineering, National Taiwan Ocean University, Keelung 20224, Taiwan, ROC
[b] Department of Marine Engineering, National Taiwan Ocean University, Keelung 20224, Taiwan, ROC
[c] Engineering and Construction Division, Formosa Petrochemical Corporation, Taiwan, ROC

Received 7 May 2004; received in revised form 24 September 2004
Available online 13 March 2005

Abstract

This study presents the thermal characteristics of a fin with excavation at base when various types of boiling occur simultaneously at adjacent locations on its surface experimentally and analytically. The heat transfer coefficient of each boiling mode is taken as a power function of wall superheat. Continuity of temperature and the heat transfer rate at the intersection of the two different modes on fin surface are employed to obtain the one-dimensional temperature distribution and total heat transfer of the excavated fin. Both heating and cooling cases are investigated in the analysis. Compared with solid pin fins, the proposed fins can extend the operating condition to a higher temperature of the heat transfer surface. In addition, the experimental data compare favorably with the analytical results.

Keywords: Excavated fin; Multi-boiling; Analytical; Experiment

1. Introduction

Recently, the study of fins in boiling liquid has been increasing enormously. Many papers [1–4] analytically investigated single boiling mode on an extended surface. This was due to the difficulty in obtaining the temperature distribution when a fin was subject to the boiling liquids with the character of high nonlinearity. However, in some applications, various heat transfer modes such as convection, nucleate boiling, transition boiling, and film boiling might occur simultaneously on a long fin depending on the designed operating conditions. Therefore, other researchers [5–7] tried to explore this problem of multi-boiling heat transfer modes coexisted on a fin numerically or experimentally.

In the analytical study of multi-boiling from a fin, Lai and Hsu [8] presented a one-dimensional model to study the heat transfer characteristics of a fin partly cooled by nucleate boiling and partly by convection. Good agreements were observed between their results and the experimental data of Haley and Westwater [5]. Lately, employing hypergeometric functions, Liaw and Yeh [9] have presented a solution procedure to obtain the temperature distribution and the heat transfer rate of a fin when various types of boiling occur simultaneously at adjacent locations on its surface. In addition, the results were verified with their own data using copper pin fins subjected to saturated water and isopropyl alcohol. Moreover, Hsu and Graham [10] also pointed out that long fins may be used to avoid the system burnout as the temperature of heat transfer surface is high in the

* Corresponding author. Tel.: +886 2 24622192; fax: +886 2 24633765.
E-mail address: rhyeh@mail.ntou.edu.tw (R.-H. Yeh).

0017-9310/$ - see front matter © 2005 Elsevier Ltd. All rights reserved.
doi:10.1016/j.ijheatmasstransfer.2004.11.026

Nomenclature

A	cross-section of fin
a	defined in Eq. (1) and given in Table 1
D	fin diameter
d	hole diameter
F	hypergeometric function
h	heat transfer coefficient, Eq. (1)
k	thermal conductivity of fin
L	length of fin
L_j	length of partitioned fin
l	depth of hole
m	power-law exponent, Eq. (1)
N	fin parameter
P	periphery of fin
Q	dimensionless temperature gradient, Eq. (4b)
Q^*	heat transfer rate of fin
q	heat flux
T	temperature
X	dimensionless coordinate, Fig. 1

Greek symbols

β	defined in Eq. (7)
ΔT	wall superheat
θ	dimensionless temperature

Subscripts

b	fin base
in	incipience of nucleate boiling
j	a chosen section of a fin
k	last section, Fig. 1
max	maximum
min	minimum
s	saturated
0	right boundary of j-section
1	left boundary of j-section

film boiling regime. In this case, the heat exchanger could be ponderous or bulky.

To make the heat exchanger more compact and practical, many investigators [11–13] showed that a higher heat transfer rate may be achieved by applying a prescribed thickness of insulation to a smaller fin at high operating temperatures. As for the optimization of fins, Haley and Westwater [5] proposed a turnip-shape fin with minimum volume for boiling heat transfer. Later, Cash et al. [14] modified the complex shape fin by using a two-cone assembly attached to a small cylindrical neck. Due to the impermanence of the insulation material and the difficulty in manufacture of these fins, lots of efforts were still needed in the improvement of the fin designs. From a practical point of view, multiple-fin arrays are used in applications of boiling heat transfer. Under this circumstances, the fin spacing design become very important because vapor trapped beneath a row of fins may cause a reduction of heat dissipation of fins. Furthermore, the bubble size and the volume of vapor produced all depend on the thermal properties of working liquid. Using cylindrical pin fins (25.4 mm$L$ × 6.3 mm$D$), Klein and Westwater [15] performed a boiling experiment of fin arrays in Freon-113. They found that a horizontal spacing of 1.6 mm is wide enough to allow all fins to act independently of each other for an array of nine fins occupying three rows. For an extended surface, a smaller cross-section may leads to a larger conductive thermal resistance. By simply drilling a hole at fin base, the temperature will drop quickly along the fin surface and it is possible to alter the boiling regime from film boiling to nucleate boiling where higher heat transfer rates can be obtained. Liaw and Yeh [16] obtained a two-dimensional temperature distribution of this fin numerically. Moreover, based on their computational results, a simple formula was also developed to predict the burnout temperature. Therefore, this application was particularly attractive for a high heat-transfer surface temperature.

The purpose of this study is thus to present the thermal characteristics of a pin fin with excavation at the center of fin base. The heat transfer process is governed by power-law-type dependence on temperature superheat. In addition, the coexistence of all the boiling modes such as film boiling, transition boiling, nucleate boiling, and free convection is considered. The total heat transfer and burnout temperature of the proposed fins are investigated. Finally, an experiment is conducted to verify the theoretical results.

2. Analytical approach

2.1. Analysis

A schematic diagram of the proposed fin subject to many types of boiling heat transfer mode is shown in Fig. 1. The fin is designed to extrude into a pool of saturated liquid. The energy from the base is conducted to the fin and is utilized in heating the adjacent boiling liquid through the lateral and end surface of the fin. The heat transfer coefficient, h, varies depending on ΔT, the temperature difference between the fin wall and the ambient liquid. The expression of h in the j-section of the fin as shown in Fig. 1 is expressed as

$$h_j(\Delta T) = a_j \cdot \Delta T_j^{m_j - 1} \tag{1}$$

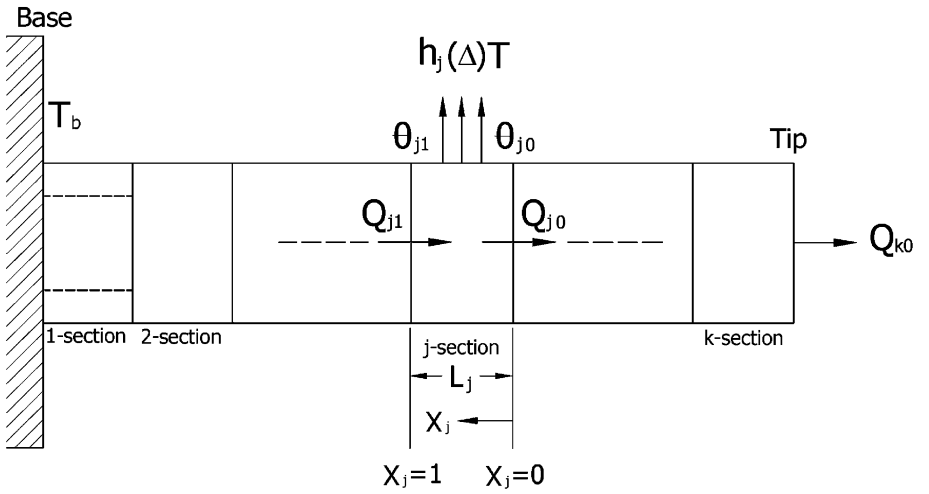

Fig. 1. Configuration of the proposed fin with excavation at fin base.

In the Eq. (1), a_j and m_j are constants depending on boiling heat transfer modes in each section and vary from one section to another. The steady state one-dimensional heat conduction equation for one segment (section) becomes

$$\frac{d^2\theta}{dX_j^2} - N_j^2 \cdot \theta_j^m = 0 \tag{2}$$

where the fin parameter, N_j, is defined as

$$N_j = L_j \cdot \sqrt{Ph_{j1}/(kA)} \tag{3}$$

and $X_j = x_j/L_j$ and $\theta_j = \Delta T_j/\Delta T_{j1}$. Note that A equals $\pi(D^2 - d^2)/4$ in an excavated portion segment and is $\pi D^2/4$ in a solid portion segment of the fin. At the two ends of one fin segment, the boundary conditions are respectively given as

$$\theta_{j1} = 1 \tag{4a}$$

$$\frac{d\theta_j}{dX_j}(0) = Q_{j0} \tag{4b}$$

where Q_{j0} is dimensionless temperature gradient at the right end of a fin section and is equal to $L_j q_0/[k(T_{j1} - T_s)]$. The temperature distribution in the j-section can be obtained by integrating Eq. (2) and using boundary conditions (4a) and (4b). For the heat transfer modes of convection, nucleate boiling, and film boiling, it is obtained as [4]

$$\begin{aligned} N_j \cdot X_j = {} & \sqrt{\frac{2}{m_j+1}(\theta_j^{-m_j+1} - \theta_j^{-2m_j}\beta^{-1})} \\ & \cdot F\left[1, \frac{m_j}{m_j+1}; \frac{3}{2}; 1 - \beta \cdot \theta_j^{-m_j-1}\right] \\ & - Q_{j0} \cdot N_j^{-1} \cdot \theta_{j0}^{-m_j} \cdot F\left[1, \frac{m_j}{m_j+1}; \frac{3}{2}; 1 - \beta \cdot \theta_{j0}^{-m_j-1}\right] \end{aligned} \tag{5}$$

and

$$\begin{aligned} N_j \cdot X_j = {} & \sqrt{\frac{2}{m_j+1}(\theta_j^{-m_j+1} \cdot \beta^{-2} - \beta^{-1})} \\ & \cdot F\left[1, \frac{m_j+3}{2(m_j+1)}; \frac{3}{2}; 1 - \beta^{-1} \cdot \theta_j^{m_j+1}\right] \\ & - Q_{j0} \cdot N_j^{-1} \cdot \theta_{j0}^{-m_j} \\ & \cdot \beta^{-1} F\left[1, \frac{m_j+3}{2(m_j+1)}; \frac{3}{2}; 1 - \beta^{-1} \cdot \theta_{j0}^{m_j+1}\right] \end{aligned} \tag{6}$$

for transition boiling mode only. In Eqs. (5) and (6), F represents hypergeometric function and β is denoted as

$$\beta = \theta_{j0}^{m_j+1} - \frac{(m_j+1)}{2} \cdot N_j^{-2} \cdot Q_{j0}^2 \tag{7}$$

The heat transfer rate at the left boundary of j-section, Q_{j1}, is derived as

$$Q_{j1} = \sqrt{\frac{2}{m_j+1} \cdot N_j^2 \cdot (1 - \theta_{j0}^{m_j+1}) + Q_{j0}^2} \tag{8}$$

The continuity equations of temperature and heat flux at the intersection of two neighboring elements are used and are written as

$$(\Delta T_j)_0 = (\Delta T_{j+1})_1 \tag{9}$$

$$(Q_j \cdot \Delta T_j/L_j)_0 = (Q_{j+1} \cdot \Delta T_{j+1}/L_{j+1})_1 \tag{10}$$

Also, note that several cases may occur at the right end of the fin. If the segment is in the mid-section of the fin, then the heat transfer from this end is designated as Q_{j0}. This is given in Eq. (4b). And if the right end of the section is exposed to ambient liquid, using the energy balance at tip, i.e. $k\frac{dT}{dx_k}(0) = a_k \Delta T_{k0}^{m_k}$ and the definition of

dimensionless temperature $\theta_{k0}^{m_k} = (\Delta T_{k0}/\Delta T_{k1})^{m_k}$, the dimensionless temperature gradient at free end becomes

$$\frac{\mathrm{d}\theta_k}{\mathrm{d}X_k}(0) = \frac{L_k}{k} \cdot h_{k1} \cdot \theta_{k0}^{m_k} \tag{11}$$

where $h_{k1} = a_k \Delta T_{k1}^{m_k - 1}$. In case of an insulated end, it leads to $\frac{\mathrm{d}\theta_k}{\mathrm{d}X_k}(0) = 0$.

2.2. Solution procedures

Because of the coexistence of multi-boiling modes on the finned surface, the fin is subdivided into many segments depending on the type of boiling. In this study, the relationship between heat flux and temperature superheat, namely q versus ΔT, is quoted from the data of Bui [17]. The superheat at the incipience of nucleate boiling is 4.4 K, and the maximum and minimum wall superheats on the boiling curve are at 18.5 K and 72 K, respectively. A set of approximate power-law functions of surface heat flux is herein listed in Table 1. A proper value of a and m is selected and used during the calculation depending on the ΔT of the finned surface.

The temperature distribution and heat transfer rate of the proposed fin are obtained by iterative method. The calculation starts from the segment at free end and proceeds toward the segment at base of the fin. First, the tip temperature (θ_{k0}) of the fin is guessed. Since the temperature at the junction of two segments is known, the segment length and heat transfer rate in the k-section can be calculated from Eqs. (4), (5), (8) and (11). In case the fin tip is subject to transition boiling, Eq. (6) is used instead of Eq. (5). Then the length and heat transfer of the neighboring segment are obtained in the same way consecutively until all the lengths of different heat transfer modes on the fin are determined. Subsequently, the next guess in tip temperature is made based on the deviation of the calculated total length and the actual fin length. The computation continues until the relative error of the two lengths is less than 10^{-4}.

3. Experiments

The apparatus used in this study is designed to permit measurements of temperatures and simultaneous observation of a fin in boiling conditions. It includes the test chamber and cooling water loop, the assembly of test piece, the preheater and gaseous nitrogen supply line. The frame of the test chamber is manufactured by welding stainless steel of 5 mm in thickness. The inside space of the test chamber is 150 mm long, 150 mm wide, and 250 mm high. The openings at four sides are 110 mm by 210 mm. Three of them are installed with 5 mm thick pyrex glasses (120 mm × 220 mm). Five-millimeter rubber stripe is placed between the pyrex glass and the stainless frame to prevent the leakage of working liquid. All the layers are compressed to fasten tightly by ten stainless steel bolts. Through the pyrex glasses the boiling phenomena can be observed. The remaining side is fitted with the assembly of the test piece. An immersion heater (250 W/110 V) controlled by a variac and located at the bottom of the test chamber is used to maintain the liquid at saturation temperature. The temperature of the liquid pool is measured by a set of thermocouples, one thermocouple is placed in the chamber about 50 mm above the test piece and another movable thermocouple at random locations. The top of the test chamber is linked with a 250 mm high rectangular stainless chimney. At the top of the chimney, a condenser, copper tube with inside diameter of 8 mm, is equipped and cold water is allowed to pass through the cooling coil. It condenses the saturated vapor to liquid state then returns it to the test chamber.

The pyrex glass jar with a heater (750 W/110 V) at the bottom is used to preheat the working liquid to saturation state and to dissolve the gas originally contained in the working liquid. During each run, the working fluid is boiled vigorously in the jar for more than 30 min and then passes the drain valve to the bottom of the test chamber. All the piping is well insulated to diminish the heat loss.

The schematic diagram of the experimental apparatus is shown in Fig. 2. In addition, detailed dimensions of the test piece as well as the heating assembly are displayed in Fig. 3. The test fin was machined from a commercially pure copper (99.99%) rod. One end is subject to boiling liquid for test. The other end of the test rod connects tightly with a large copper block (120 mm × 120 mm × 120 mm). In addition, the copper block is drilled to fit twelve cartridge heaters (500 W/220 V each). Two sets of variac are used to regulate the input power from the cartridge heaters. Fiberglass block are used as the insulation material to achieve an isothermal condition at the fin base. In addition, the square heating block is wrapped with several layers of ceramic fiber to diminish the heat loss. Teflon gasket ring, insulation material, is sealed between the glass fiber and the wall of the test chamber. Around the Teflon ring the gap is sealed with high-temperature resistant silicon sealant which is used to prevent the working liquid from leaking.

Table 1
Correlations of surface heat flux

Heat transfer modes	a	m	ΔT
Convection	1402	1.33	$0 \leqq \Delta T < 4.4$ K
Nucleate boiling	157.6	2.81	4.4 K $\leqq \Delta T <$ 18.5 K
Transition boiling	7.55×10^8	−2.46	18.5 K $\leqq \Delta T <$ 72 K
Film boiling	3100	0.5	72 K $\leqq \Delta T$

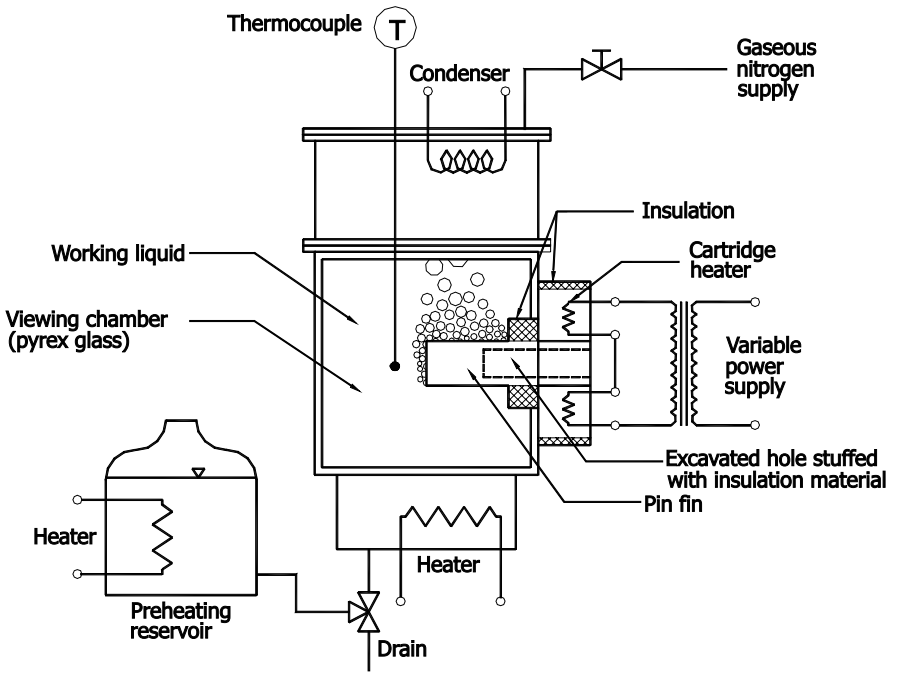

Fig. 2. Schematic diagram of the experimental apparatus.

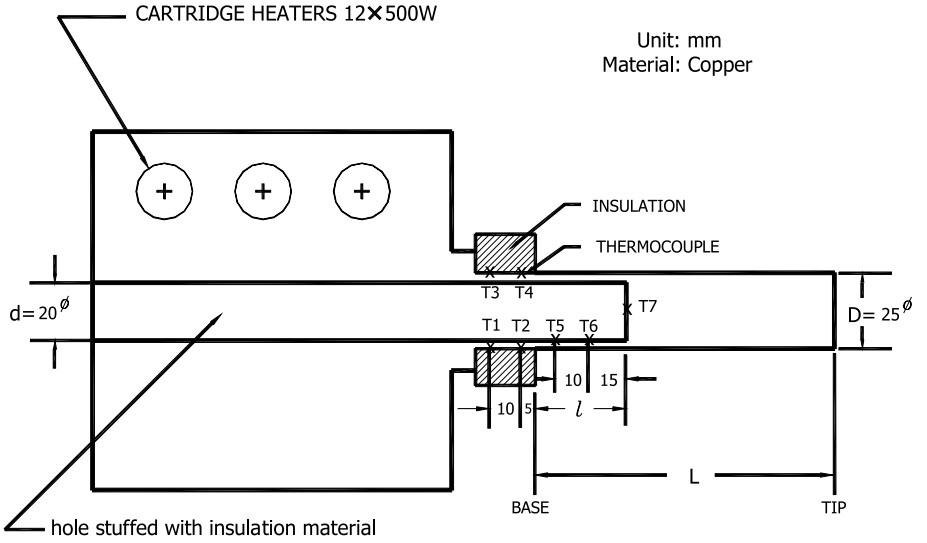

Fig. 3. Details of the test assembly and locations of thermocouples.

It is noted that seven chromel–alumel thermocouples (K-type, 30 gage) are positioned as displayed in Fig. 3. The outputs of the thermocouples were recorded by a data recorder (Yokogawa model HR-2500). An auto-transformer with voltage power stabilizer is used to guarantee the recorder running correctly. In a heating test, as the temperature at the base of the fin is first increased above the boiling point, a few nucleation sites become active at the fin base and free convection covers the remainder of the fin. By slowly increasing the voltage input of the cartridge heaters, film boiling will occur at the base of the fin and four different heat transfer modes are shown in a stable configuration on the finned surface. Continuously increasing in the base temperature, the regions of the peak heat flux, transition and nucleate boiling, move toward the tip of fin. For cooling tests,

ΔT_b is initially heated to a superheat of 350 K with continuous charging gaseous nitrogen to the test chamber to avoid oxidation of fins. In this case, the whole fin is governed by film boiling. The power input is decreased step by step after it reaches a steady state. The procedure continues until vapor film collapses on the finned surface.

4. Results and discussion

First of all, cylindrical pin fins with or without excavation at fin base are investigated analytically. Fig. 4 depicts the effects of the excavated-hole diameters on the heat transfer rate of the fins. An analytical solution of a solid pin fin [9] is included in this figure for comparison. Similar to previous work [9], a hysteresis region is found, i.e. there are two solutions at a certain range of ΔT_b. It is noted that the proposed fins are effective in raising the burnout temperature of the system. In a heating case, the burnout temperature of a solid pin fin with a diameter of 20 mm and a length of 100 mm is $\Delta T_b = 395$ K whereas it rises to $\Delta T_b = 415$ K for $l = 20$ mm and $d/D = 0.5$, and even extends to a fin base wall superheat of 594 K for $l = 20$ mm and $d/D = 0.8$. When $\Delta T_b \gg \Delta T_{min}$, the wall surface is entirely in film boiling regime. Since the cross-section of a fin is inversely proportional to the thermal resistance, a larger temperature drop may be achieved by increasing d/D and the nucleate and transition boiling will possibly move in and spread over a wider area of the finned surface. Apparently, the burnout temperature is higher for a larger d/D at fixed l. Nevertheless, it is worthwhile to mention that the proposed excavated fins are not suitable for a lower wall temperature because of smaller heat transfer rates compared with solid pin fins. In a cooling case, it is also observed that the film-collapse temperature is higher for a larger d/D. The destabilization of film boiling is useful in some situations. For instance, it can increase the cooling rate of a workpiece during a tempering process.

A further study of the temperature profiles of the proposed excavated fins is given in the Fig. 5 for a heating case. In this figure, ΔT_{min} (=72 K), ΔT_{max} (=18.5 K), and ΔT_{in} (=4.4 K) are given for reference. It is known that ΔT_{min}, T_{max} and ΔT_{in} are minimum wall superheat, maximum wall superheat and the superheat at the incipience of nucleate boiling, respectively. When the fin tip temperature is greater than ΔT_{min}, the whole finned surface will be completely blanketed with vapor and subject to film boiling only. When the tip temperature drops to a value between ΔT_{min} and ΔT_{max}, the working liquid will break the vapor film at the tip of the fin and passes through the thin film to hit the heating surface. Transition boiling takes place on free end of the fin. As $\Delta T_b > \Delta T_{in}$, a few bubbles begin to show up on the nucleation sites of the finned surface. It is observed that the whole fin is in film boiling region for a solid pin fin at $\Delta T_b = 450$ K. The temperatures of the finned surface drop a little when $l = 20$ mm and $d = 10$ mm, in this case the fin is still subject to film boiling. As the ratio, d/D, of the fin is increased to 0.75, larger temperature drop is observed and transition and nucleate boiling begin to occur and coexist on the fin simultaneously. Note that the temperature curves are not so smooth for $d/D = 0.75$ and 0.8. This is due to the fact that the fin

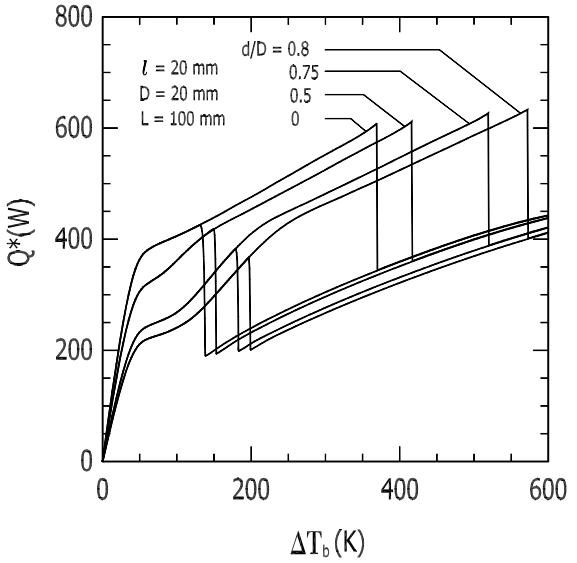

Fig. 4. Dependence of heat dissipation on fin base temperature for various hole diameters.

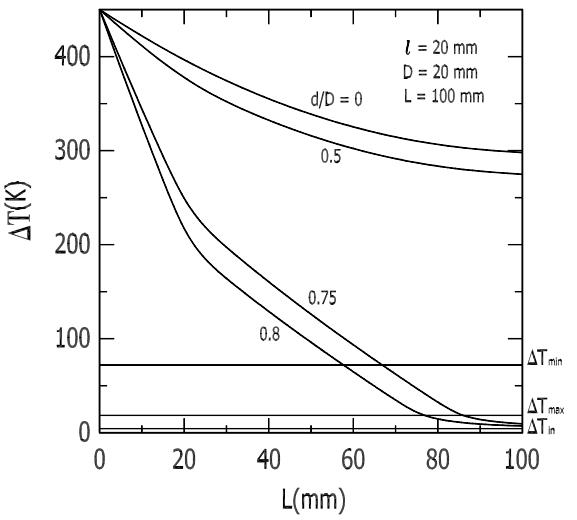

Fig. 5. Temperature distributions of the proposed fins at $\Delta T_b = 450$ K for heating runs.

parameter, N_j, with excavation is different from that without one. The temperature gradient will then be different although the 1 and 2 segments near the fin base may be both in the same boiling heat transfer mode. The temperature drops abruptly in the first 20 mm, 1-section, of the fin because of the depth of the larger hole. Although the subsequent 2-section is in the film boiling, its temperature gradient is the same as 3-section, transition boiling, for the continuity of temperature and heat flux at two adjacent sections. The tip temperatures reduce to the superheats at about the incipience of nucleate boiling for $d/D = 0.75$ and 0.8 fins. The slopes of temperature profiles thus become smaller for these end sections. In a cooling case, the temperature distributions of the 100 mm long fins for $\Delta T_b = 160$ K are displayed in Fig. 6. Four different heat transfer modes such as film boiling, transition boiling, nucleate boiling and convection occur simultaneously on the fins for $d/D = 0.75$ and 0.8. Generally, it is difficult to control the tip temperature of a fin to fall in transition boiling mode. However, Bui and Dhir [18] and Liaw and Yeh [9] observed the transition boiling of water on a vertical surface and fin's end surface near minimum superheat, respectively. For a fin with tip temperature around ΔT_{min}, while increasing d/D, the thermal resistance in the proposed fin becomes large and the steady-state tip temperature will soon drop below ΔT_{max}. The entire finned surface is thus occupied by the four different heat transfer modes.

Fig. 7 shows the effects of hole depth on the heat duty of the excavated fins for $d/D = 0.5$. Similar phenomena are observed both in heating and cooling cases. The deeper the excavation is, the higher the burnout temperature and the film-collapse temperature will be for a fixed hole diameter at fin base. This is due to the fact that the smaller the cross-section is, the large the conductive thermal resistance is in an extended surface. The high temperature region can be shortened by using a deeper hole at fin base so that the temperature drop required to pass film boiling can be achieved in a short distance. In this case, the whole fin governed by film boiling will then occur at a higher temperature. On the other hand, the excavated hole on a fin results in a lower tip temperature than that of a solid one. While cooling, the highly efficient transition and nucleate boiling will easily move in for a deep hole from the fin tip at a higher ΔT_b. Also note that differing from the solid pin fin, the increases in heat duty of the excavated fins are not so smooth at increasing ΔT_b. This is mainly caused by the different depths of the holes and can be understood from the investigation of Fig. 8. In this figure, the temperature profiles for 100 mm long fins are displayed for $d/D = 0$ and 0.5. Note that compared with a solid pin fin, the temperature gradient at fin base is larger at a higher ΔT_b for the excavated fin with $d/D = 0.5$ and $l = 60$ mm. For the solid fins, constant temperature gradient at fin base is observed at different ΔT_b, whereas the slopes of the temperature profiles at fin base increase with increasing ΔT_b for the proposed fins. This can be explained from the fact that the temperature drop is larger and most of the finned surface near the tip is subject to free convection for the proposed excavated fin. In this case, four different heat transfer modes, i.e. film boiling, transition boiling, nucleate boiling, and convection simultaneously show up on the fin. For a solid pin fin, only three boiling heat transfer modes occur on the

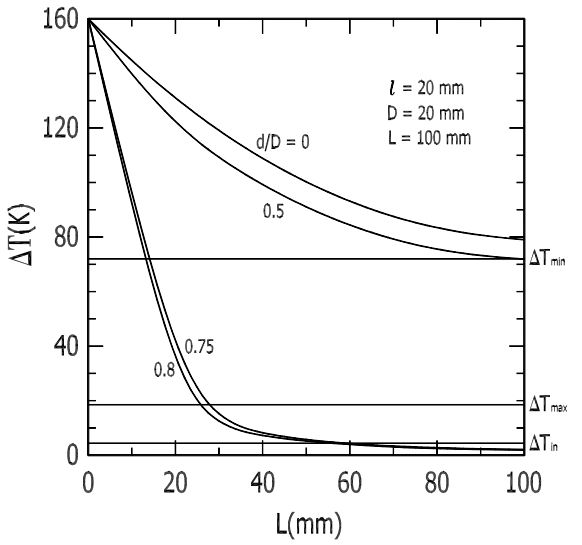

Fig. 6. Temperature distributions of the proposed fins at $\Delta T_b = 160$ K for cooling runs.

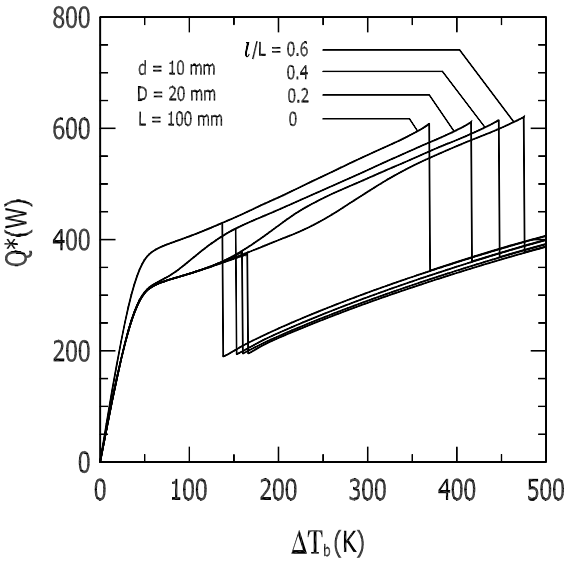

Fig. 7. Dependence of heat dissipation on fin base temperature for various hole depths.

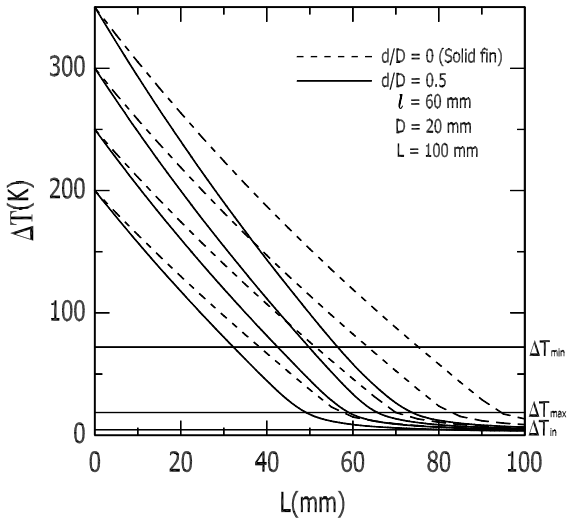

Fig. 8. Comparisons of temperature profiles between the solid pin fins and the proposed fins for ΔT_b = 200 K, 250 K, 300 K, and 350 K.

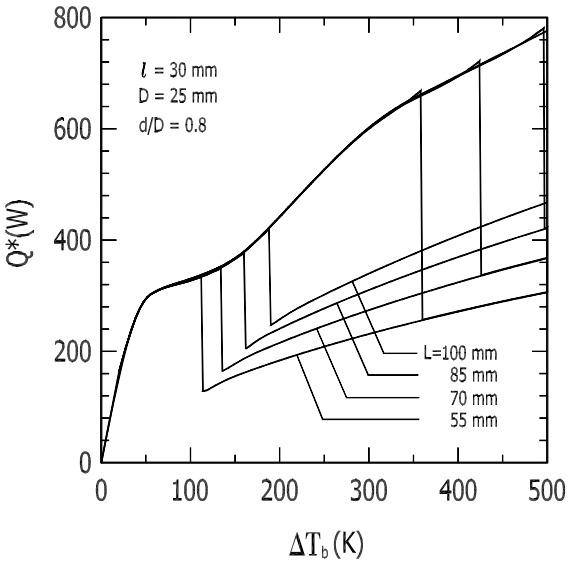

Fig. 9. Dependence of heat dissipation on fin base temperature for various fin lengths.

finned surface at the same ΔT_b. As ΔT_b increases, free convection will be eventually pushed off the fin tip and efficient nucleate boiling mode will cover most of the fin around the free end. An apparent raise of heat dissipation at a certain range of ΔT_b for the proposed fin is therefore shown. It is evident that the diameter and depth of hole can effectively raise the burnout superheats especially when the heat exchanger is operated at a very high temperature. Therefore, it is recommended that the raise of burnout temperature can be readily achieved by widening the hole at fin base for a stubby fin and by deepening the hole for a slender fin.

It is worthwhile to investigate the effects of fin length on a fixed size of hole at fin base. Fig. 9 displays the dependence of heat dissipation on ΔT_b at a fixed hole size for L = 55 mm, 70 mm, 85 mm, and 100 mm. It is observed that both the burnout and film-collapse temperatures are higher for a longer fin. Also note that the burnout temperature for L = 85 mm is close to ΔT_b = 500 K and the burnout superheat for L = 100 mm is too high and is not included in this figure. The main purpose of the excavation at fin base is to shift the safety operating limit to a higher ΔT_b.

However, in comparison with the bare surface, the advantage of using fins in boiling heat transfer is obviously not only to enhance heat transfer but also to broaden the safety operating temperature. The effects and thermal behavior mechanism of the fin length on the temperature jump were explored extensively in the author's previous work [9].

A few experiments are also conducted for the excavated fins with d/D = 0.8. Fig. 10 presents the heat duty for various excavated fins at different base wall super-

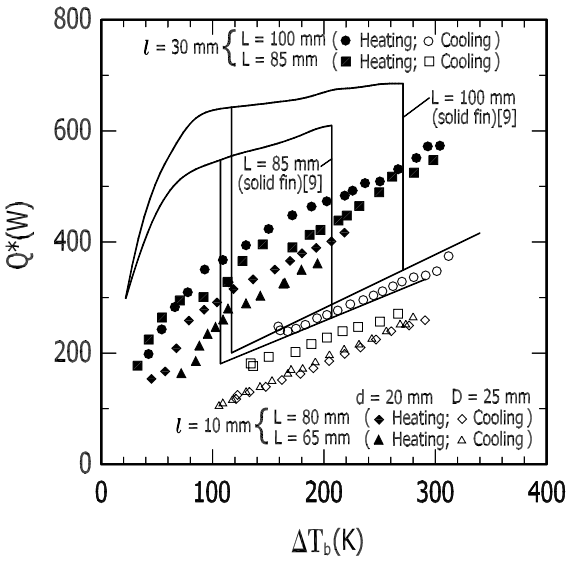

Fig. 10. Experimental data for the heat transfer rates of the proposed fins and previous work[9].

heats. Note the experimental data of solid pin fins for L = 85 mm and 100 mm are given for comparison in this figure. For a given ΔT_b, the heat duties for heating runs are mostly higher than those of cooling runs. From Fig. 10, the heat transfer rates of the proposed fins increase with fin length. The effects of the hole depth is insignificant due to the whole fins are mainly subject to nucleate and transition boiling for low ΔT_b in heating tests. No burnout is observed for the excavated fin with

$L = 85$ mm and 100 mm at the burnout temperatures of the solid pin fins. This signifies that the burnout temperature of the proposed fin is higher that of an ordinary pin fin. A common trait is observed that when burnout is about to occur, the tip temperature will fall around maximum superheat. Once the nucleate boiling disappears from fin tip, transition boiling is instantaneously pushed off and the whole fin is then subject to low heat flux (film boiling) region. To avoid the damage of the heater, the experiment ends after the heater temperature or the input voltage reaches the prescribed safety limits. For cooling runs, both the heat duty of fins and the minimum wall superheat increase with fin length. Note that for excavated fins with a hole of $l = 30$ mm, $d = 20$ mm, the film-collapse temperatures extend from 107 K to 144 K for $L = 85$ mm and from 117 K to 163 K for $L = 100$ mm in comparison with the solid fins. This phenomenon is identical to the description of the analytical results as stated previously. The tip temperature of a fin drops to minimum superheat when the vapor film at the free end portion is about to collapse.

Figs. 11 and 12 show the comparison of predicted and measured heat transfer rates for $L = 85$ mm and 100 mm. It is worthwhile to mention that the predicted burnout temperatures for the excavated fins are superheats of 492 K and 574 K for $L = 85$ mm and 100 mm respectively which are not shown in the figures in heating runs. The predicted film-collapse temperatures are about 30 K and 35 K higher than the measured values for $L = 85$ mm and 100 mm in cooling process. This may be the reason that the boiling curve used in the theoretical analysis is obtained from the experimental data on a flat plate [18], which is different from that on a rod. From the observation of the experiment, burnout occurs when transition and nucleate boiling are pushed off the fin tip and film-collapse takes place when transition and nucleate boiling show up around the tip. Therefore, it is suspected that the present one-dimensional model can not accurately predict the temperature jump especially when the hole diameter is large or when the tip surface is subject to high heat flux regions (nucleate or transition boiling). On the whole, the model predictions in heat dissipations of fins compare favorably with the experimental data.

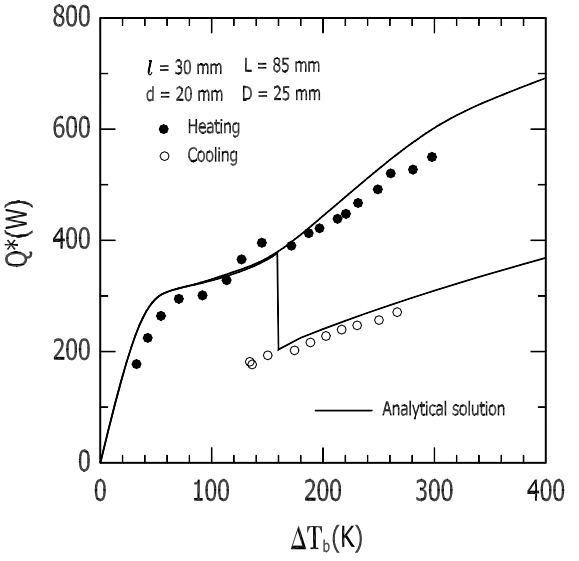

Fig. 11. Comparison of predicted and measured heat transfer rates for the proposed fins in heating and cooling runs. ($L = 85$ mm, $D = 25$ mm; $l = 30$ mm, $d = 20$ mm).

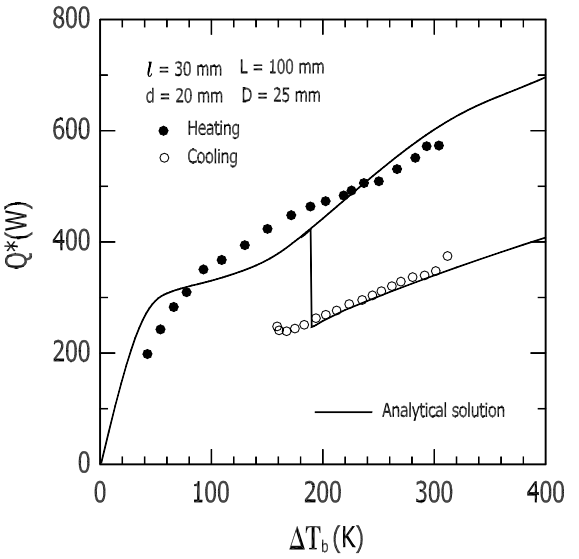

Fig. 12. Comparison of predicted and measured heat transfer rates for the proposed fins in heating and cooling runs. ($L = 100$ mm, $D = 25$ mm; $l = 30$ mm, $d = 20$ mm).

5. Conclusions

In this study, the thermal characteristics of excavated fins are investigated analytically and experimentally for boiling heat transfer. The dimensions of hole at center base of fins are taken into consideration. From the foregoing results, it can be concluded as follows:

1. The lengths of different heat transfer modes are calculated when multi-type boiling coexists on an excavated fin. In addition, the temperature distribution and heat transfer rate of the fin are predicted by the present model.
2. The critical temperatures, both burnout and film-collapse temperatures, obtained for the proposed fins are higher than those of solid ones.

3. For a fixed hole diameter, the deeper the hole is, the higher the critical temperatures are for the proposed excavated fin. Similarly, the larger the hole diameter is, the higher the critical temperatures are for a fixed depth of hole.
4. Experiments are conducted for fins with different dimensions of holes in saturated water. The experimental data of fins' heat duty compare favorably with theoretical predictions.

Acknowledgement

This work was supported in part by the National Science Council of Taiwan, Republic of China through contract no. NSC 81-0401-E019-01.

References

[1] A.K. Sen, S. Trinh, An exact solution for the rate of heat transfer from a rectangular fin governed by a power law-type temperature dependence, J. Heat Transfer 108 (1986) 457–459.
[2] H.C. Unal, Temperature distributions in fins with uniform and non-uniform heat generation and non-uniform heat transfer coefficient, Int. J. Heat Mass Transfer 30 (1987) 1465–1477.
[3] R.H. Yeh, S.P. Liaw, An exact solution for thermal characteristics of fins with power-law heat transfer coefficient, Int. Commun. Heat Mass Transfer 17 (1990) 317–330.
[4] S.P. Liaw, R.H. Yeh, Fins with temperature dependent surface heat flux-I. Single heat transfer mode, Int. J. Heat Mass Transfer 37 (1994) 1509–1516.
[5] K.W. Haley, J.W. Westwater, Boiling heat transfer from single fins, Proc. 3rd Int. Heat Transfer Conf., Chicago, vol. 3, 1966, pp. 245–253.
[6] I.N. Dul'kin, N.I. Rakushina, L.I. Royzen, V.G. Fastovskiy, Heat transfer with water and freon-113 boiling on a non-isothermal surface, Heat Transfer—Soviet Research 3 (1971) 61–69.
[7] B.S. Petukhov, S.A. Kovalev, W.M. Zhukov, G.M. Kazakov, Study of heat transfer during the boiling of a liquid on the surface of a single fin, Heat Transfer—Soviet Research 4 (1972) 148–156.
[8] F.S. Lai, Y.Y. Hsu, Temperature distribution in a fin partially cooled by nucleate boiling, AIChE J. 13 (1967) 817–821.
[9] S.P. Liaw, R.H. Yeh, Fins with temperature dependent surface heat flux-II. Multi-boiling heat transfer, Int. J. Heat Mass Transfer 37 (1994) 1517–1524.
[10] Y.Y. Hsu, R.W. Graham, Transport Process in Boiling and Two-phase Systems, McGraw-Hill, New York, 1976, p. 439.
[11] C.W. Cowley, W.J. Timson, J.A. Sawdye, A method for improving heat transfer to a boiling liquid, Ind. Eng. Chem. Proc. Des. Dev. 1 (1962) 82–84.
[12] G.R. Rubin, L.I. Royzen, I.N. Dul'kin, Heat transfer in liquid boiling on insulated-coated fins, Heat Transfer—Soviet Research 3 (1971) 130–134.
[13] C.C. Shih, J.W. Westwater, Use of coatings of low thermal conductivity to improve fins used in boiling liquids, Int. J. Heat Mass Transfer 15 (1972) 1965–1968.
[14] D.R. Cash, G.J. Klein, J.W. Westwater, Approximate optimum fin design for boiling heat transfer, J. Heat Transfer 93 (1971) 19–24.
[15] G.J. Klein, J.W. Westwater, Heat transfer from multiple spines to boiling liquids, AIChE J. 17 (1971) 1050–1056.
[16] S.P. Liaw, R.H. Yeh, Boiling heat transfer from an excavated fin, Int. Commun. Heat Mass Transfer 19 (1992) 215–228.
[17] T.D. Bui, Film and Transition Boiling Heat Transfer on an Isothermal Vertical Surface, Ph.D. Thesis, University of California, Los Angeles, California, 1984.
[18] T.D. Bui, V.K. Dhir, Transition boiling heat transfer on a vertical surface, J. Heat Transfer 107 (1985) 756–763.